Quality Improvement Study

Medicine®

OPEN

CBCT-based 3D MRA and angiographic image fusion and MRA image navigation for neuro interventions

Qiang Zhang, MD[a], Zhiqiang Zhang, MD[a], Jiakang Yang, MD[b], Qi Sun, PhD[c], Yongchun Luo, MD[a], Tonghui Shan[a], Hao Zhang[a], Jingfeng Han, PhD[c], Chunyang Liang, MD[a], Wenlong Pan[a], Chuanqi Gu[a], Gengsheng Mao, MD[d,*], Ruxiang Xu, MD[a,*]

Abstract

Digital subtracted angiography (DSA) remains the gold standard for diagnosis of cerebral vascular diseases and provides intraprocedural guidance. This practice involves extensive usage of x-ray and iodinated contrast medium, which can induce side effects. In this study, we examined the accuracy of 3-dimensional (3D) registration of magnetic resonance angiography (MRA) and DSA imaging for cerebral vessels, and tested the feasibility of using preprocedural MRA for real-time guidance during endovascular procedures.

Twenty-three patients with suspected intracranial arterial lesions were enrolled. The contrast medium-enhanced 3D DSA of target vessels were acquired in 19 patients during endovascular procedures, and the images were registered with preprocedural MRA for fusion accuracy evaluation. Low-dose noncontrasted 3D angiography of the skull was performed in the other 4 patients, and registered with the MRA. The MRA was overlaid afterwards with 2D live fluoroscopy to guide endovascular procedures.

The 3D registration of the MRA and angiography demonstrated a high accuracy for vessel lesion visualization in all 19 patients examined. Moreover, MRA of the intracranial vessels, registered to the noncontrasted 3D angiography in the 4 patients, provided real-time 3D roadmap to successfully guide the endovascular procedures. Radiation dose to patients and contrast medium usage were shown to be significantly reduced.

Three-dimensional MRA and angiography fusion can accurately generate cerebral vasculature images to guide endovascular procedures. The use of the fusion technology could enhance clinical workflow while minimizing contrast medium usage and radiation dose, and hence lowering procedure risks and increasing treatment safety.

Abbreviations: 2D = two-dimensional, ACoA = anterior communicating artery, AICA = anterior inferior cerebella artery, BA = basilar artery, CBCT = cone beam computed tomography, DAVF = dural arteriovenous fistula, DSA = digital subtracted angiography, F = female, ICA = internal carotid artery, L = left, M = male, MCA = middle cerebral artery, MPR = multiplanar reconstruction, MRA = magnetic resonance angiography, MRI = magnetic resonance imaging, PCA = posterior cerebral artery, PCoA = posterior communicating artery, R = right, VA = vertebral artery, VRT = volume-rendering techniques.

Keywords: digital subtracted angiography, image fusion, intervention, magnetic resonance angiography, navigation

1. Introduction

Nowadays, flat panel detector cone-beam computed tomography (CBCT)-equipped angiographic suite has been commonly used for detection of cerebral vascular diseases and as image assistance for endovascular procedures. CBCT imaging, featured with spatial resolution up to 0.1 to 0.2 mm, enables visualization of the anatomy of the vasculature in both 2-dimensional (2D) and 3D space. Two-dimensional fluoroscopy and digital subtracted angiography (DSA) with radio opaque iodine contrast medium injection are useful in guiding catheterization procedures. Detailed morphological information of blood vessels provided by 3D DSA aids in detection of any circulatory disorder.[1–6] It has now become possible to overlay the 3D vessels onto the 2D live fluoroscopic images, which allows real-time localization of the catheter or wire position with respect to anatomical structure and visualization of such structures of interest from any desired angle. However, DSA-guided procedures requires x-ray for acquiring 2D and 3D images of the head and neck vessels, respectively, which provide adequate information on a lesion and selection of the best possible working angle, and also real-time imaging. This is associated with the potentials for long-term

Editor: Francisco Vaz-Guimaraes Filho.

The author(s) declared no potential conflicts of interest with respect to the research, authorship, and/or publication of this article.

[a] Beijing PLA Military General Hospital Affiliated Bayi Brain Hospital, Beijing, [b] The Second People's Hospital of Hefei, Hefei, [c] Siemens Ltd. China, Healthcare Sector, [d] General Hospital of Chinese People's Armed Police Forces, Beijing, China.

[*] Correspondence: Professor Ruxiang Xu, Beijing PLA Military General Hospital Affiliated Bayi Brain Hospital, No. 5, Nanmencang, Dongcheng District, Beijing 100700, China (e-mail: xuruxiang_bjjz@hotmail.com); Co-correspondence: Professor Gengsheng Mao, General Hospital of Chinese People's Armed Police Forces, No. 69, Yongding Road, Haidian District, Beijing 100039, China (e-mail: mclxmgs@126.com).

Medicine (2016) 95:32(e4358)

Received: 2 December 2015 / Received in final form: 16 June 2016 / Accepted: 1 July 2016

http://dx.doi.org/10.1097/MD.0000000000004358

health hazards resulting from prolonged ionizing radiation of the x-ray exposure to patients. Additionally, although DSA is still the gold standard for depicting cerebral vasculature and providing intraprocedural guidance, this technique involves extensive usage of iodinated contrast medium that may induce allergy and nephrotoxicity and limit DSA applications in patients with renal diseases.[7–10]

Magnetic resonance imaging (MRI) generates image sequence based on the magnetic field and radio frequency waves. MRI produces high-quality images with excellent contrast details of soft tissue and anatomic structures without exposing the patients or clinicians to ionizing radiation (x-rays). Magnetic resonance angiography (MRA), in particular, permits visualization and analysis of cerebral vessels in the brain while avoiding radiation and contrast medium injection. Although the sensitivity of MRA is generally inferior to that of conventional angiography, it has been successfully used to identify stenosis, aneurysm, arteriovenous malformations, and diagnose atherosclerosis and other vascular lesions in major cerebral vessels.[11–15]

With the rapid advancement of imaging technologies, image registration between 2 stand-alone imaging modalities can be obtained. For example, the bony references of a preprocedural MRA image can be superimposed to an intraprocedural angiographic image. The 2 image datasets are then displayed onto the live fluoroscopic image, either individually or combined.[16–18]

In this study, we first tested the feasibility and accuracy of the 3D MRA and angiographic image fusion. Secondly, we presented our initial experiences where the success of the endovascular treatment procedures benefited from the combined use of preprocedurally acquired MRA and intraprocedurally acquired angiography techniques.

2. Materials and methods

2.1. Patient selection

From May to September 2015, 23 patients with suspected neurovascular lesions were enrolled into this study. These patients were scheduled for diagnostic angiography or interventional recanalization. Detailed information of individual patient was listed in Table 1. This study was approved by the hospital ethics committee.

2.2. Preprocedural MRA image acquisition

Preprocedural MRI imaging was performed using a whole-body 3-Tesla MR scanner (Signa HDxt; GE Healthcare, Little Chalfont, UK) with an 8-channel head coil. Three-dimensional time-of-flight was applied in MRA imaging with the following parameters: fast field echo, repetition time 22 ms, echo time 3.9 ms, flip angle 15°, field of view 220 mm × 165 mm, slice thickness 1.4 mm, and total acquisition time 3 minutes 55 seconds.

2.3. Intraprocedural 3D angiographic image acquisition

Three-dimensional angiographic images were acquired during the endovascular procedures. For the first group of 19 patients, rotational x-ray angiography was performed to generate 3D vasculature. To do this, a 3D mask image was acquired first, followed by a fill run. Contrast medium (Ioversol, 320 mgI/mL) was injected during the fill run into the artery of interest by a power injector (300 psi) at an injection rate of 3 mL/s for 6 seconds, and with 1 sesond x-ray delay to ensure full contrast of the arteries. For the second group of 4 patients, no contrast medium was injected, and noncontrasted low dose 5 econds

Table 1

Patient diagnostic and treatment information.

Patient no.	Age, sex	Diseases	Symptoms
Group 1			
1	54, F	BA stenosis, R-VA occlusion	Dizziness
2	51, F	Bilateral ACA, L-MCA, R-VA stenosis	R-lower limb weakness
3	45, M	R-ICA aneurysm	Blepharoptosis
4	75, M	L-ICA intima injury	Headache and vomiting
5	51, F	Bilateral VA dissection-aneurysm	Sudden onset of headache and unconsciousness
6	36, M	R-MCA severe stenosis	Episodic headache
7	33, F	R-VA aneurysm	Headache
8	50, F	R-AICA aneurysm	Sudden onset of headache
9	59, F	R-ICA aneurysm	Intermittent headache
10	56, M	L-PCoA funnel shaped dilation	Sudden onset of headache
11	66, F	R-ICA multiple aneurysms, L-ICA aneurysm	Neck discomfort
12	63, F	L-ICA multiple aneurysms, L-DAVF	Walking unsteadiness
13	62, F	R-ICA occlusion, R-MCA stenosis	Sudden onset of L-limb weakness
14	58, M	R-ICA severe stenosis, R-ICA occlusion	Episodic syncope
15	58, F	L-VA, L-ICA aneurysms	Sudden onset of frontal headache
16	63, M	—	—
17	57, M	Bilateral MCA occlusion, bilateral ECA stenosis	Episodic dizziness
18	62, M	R-ICA aneurysm	Sudden onset of L-limb weakness and cough
19	51, F	L-meningioma	L-limb weakness, cough and dizziness
Group 2			
20	43, F	R-VA aneurysm	Sudden onset of headache and unconsciousness
21	65, F	BA occlusion	Sudden onset of unconsciousness
22	70, M	L-ACoA aneurysm	Sudden onset of headache
23	52, F	BA stenosis	Dizziness

ACoA = anterior communicating artery, AICA = anterior inferior cerebella artery, BA = basilar artery, CBCT = cone beam computed tomography, DAVF = dural arteriovenous fistula, DSA = digital subtracted angiography, F = female, ICA = internal carotid artery, L = left, M = male, MCA = middle cerebral artery, MPR = multiplanar reconstruction, MRA = magnetic resonance angiography, MRI = magnetic resonance imaging, PCA = posterior cerebral artery, PCoA = posterior communicating artery, R = right, VA = vertebral artery, VRT = volume-rendering techniques.

rotational scan was acquired. The C-arm rotated for 200° in 5 sesonds at a speed of 1.5°/frame and with x-ray dose of 0.36 μGy/frame. A total number of 133 projection images were generated as an output. The resulting raw projection images were then immediately transferred to a commercially available workstation (*syngo* X Workplace, Siemens Healthcare, Germany) for 3D volume reconstruction.

For the first group, reconstructions were performed using the reconstruction mode "native fill" to create a contrast-enhanced image showing both vessels and skull. For the second group, reconstructions were performed using the reconstruction mode "native mask" to make a native image of the skull. The kernel type was "HU," and image impression was "normal" for either group reconstructions.

2.4. 3D MRA-angiographic image fusion

The preprocedural MRA images were imported as Dicom images into the same workstation. The angiographic images acquired during the endovascular procedures were co-registered with the MRA images using commercially available functionality "*syngo* Inspace 3D/3D fusion." Both the MRA and angiographic images were presented in different colors and in the same window as orthogonal multiplanar reconstruction (MPR) images in axial, sagittal, coronal orientations, and also displayed using volume-rendering techniques (VRTs) as shown in Fig. 1. Two image datasets were fused via intensity-based automatic registration matched to the bony references (i.e., the skull) for alignment of the 2 volumes. When a registration error was detected to be significant, the re-registration would be made by manual registration of visual matching. The two 3D image volumes of different colors were superimposed to achieve fusion precision.[19] The registration matrix was then stored and applied to the fusion dataset. In the automatically opened "Dual-Volume Properties" window, only MRA image was shown. The window width and window center were adjusted to best visualize the lesion.

After an accurate 3D/3D registration was achieved between MRA and angiography, by using "*syngo* iPilot dynamic" functionality, the VRT images of the 3D MRA could then be overlaid with the live 2D fluoroscopy and displayed. A 3D live roadmap visualization of the target vessels was provided as a result during endovascular procedures. The opacity of the overlaid MRA was adjustable to receive a better contrast of the artery, guide wire, catheter, and anatomical background. The MRA image was dynamically updated in response to geometrical changes of the CBCT system such as table movement, C-arm rotations, and so on. If a misalignment was found between the fluoroscopy and the MRA, the auto-recording mode could be switched to the manual mode to perform 2D/3D manual registration based on visual matching.

3. Results

The imaging results of the first 19 patients were independently read by 2 experienced radiologists. In particular, they checked

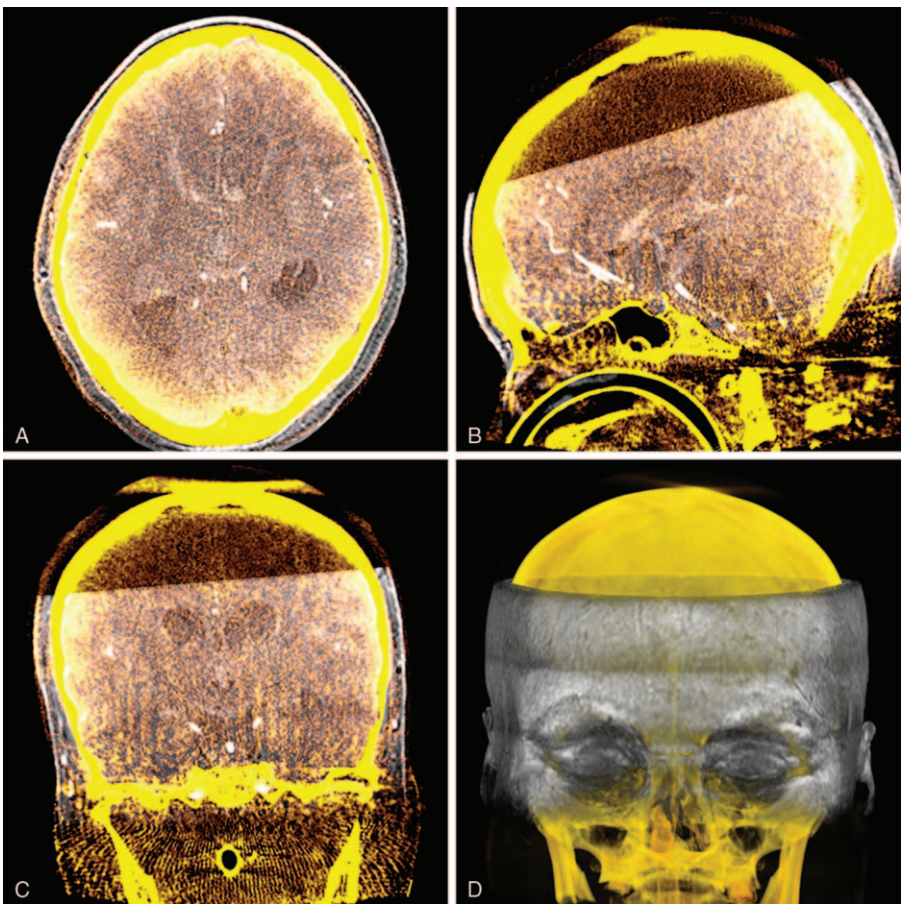

Figure 1. Three-dimensional (3D) MRA (white) and DSA (yellow) fusion images presented in axial (A), sagittal (B), coronal (C) orientations, and using VRT technique (D). DSA = digital subtracted angiography, MRA = magnetic resonance angiography, VRT = volume-rendering technique.

whether the vessels in 2 models were superimposed in the 4 windows using a 3-point rating scale, where 3 = image fusion of high accuracy without obvious misregistration, class 2 = mild to moderate image misregistration, and class 1 = severe misregistration. Differences in assessment were discussed and resolved by the consensus. The overall quality of the 3D MRA and angiographic fusion was scored as class 3 in 16 of the 19 cases and as class 2 in the other 3 cases. Deviations were found to be less than 1 mm with respect to the diameter of major vessels, and also characteristics of lesions including the size of aneurysm neck and sac, length, and diameter of stenosis. The referring radiologists and physicians concluded that the information provided by the merged MRA images was helpful for 19 operations. Representative cases are shown in Fig. 2, which illustrate accurate image fusion of the 3D MRA and angiographic datasets for different clinical scenarios including aneurysm, stenosis, and occlusion at different levels of intracranial vasculature.

The combined use of bony reference and visual matching presumably allows a precise registration of the 3D MRA with angiographic image and subsequently an accurate depiction of the intracranial vessels. This infers that the 3D MRA registered with the native skull angiography alone without additional acquisition of 3D DSA of the vessels can be used to navigate endovascular procedures. This idea was tested in the second group of 4 patients. No contrast medium was injected during the 3D angiographic acquisition, and the endovascular procedures were performed solely under the guidance of the registered 3D MRA roadmap. We did conduct a few 2D DSA acquisitions that included a 2 to 8 mL of contrast medium injection to both verify the spatial accuracy of the 3D MRA roadmap and confirm the completion of the procedures.

3.1. Representative case 1

The first representative case was shown in Fig. 3 that demonstrated the 3D anatomy of a small saccular aneurysm

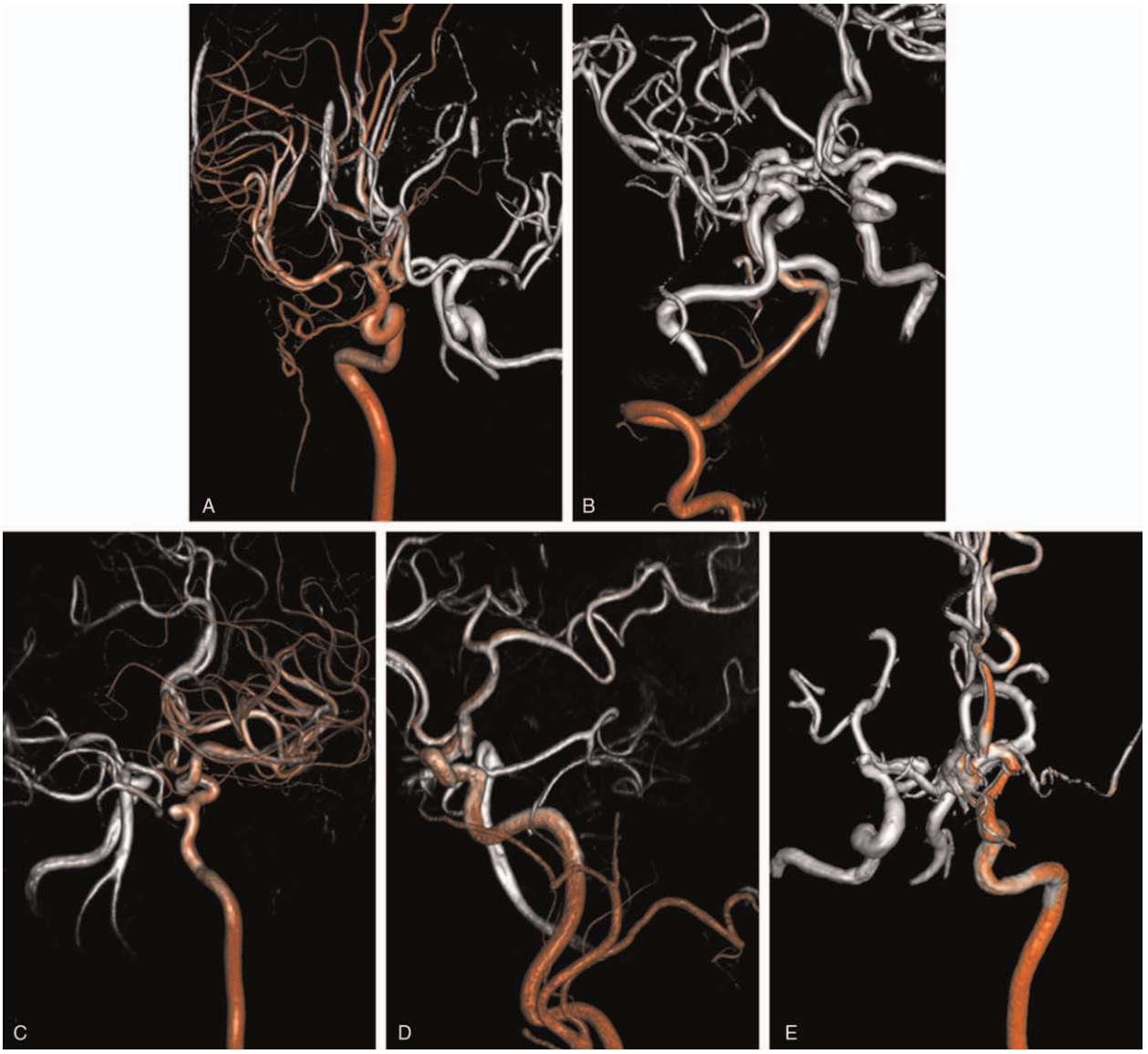

Figure 2. Three-dimensional (3D) MRA (white) and angiographic (red) fusion results of intracranial arteries: A, R-MCA stenosis; B, R-AICA aneurysm; C, R-ICA aneurysm; D, R-ICA aneurysm; E, L-MCA occlusion. L-MCA = left middle cerebral artery, MRA = magnetic resonance angiography, R-AICA = right anterior inferior cerebella artery, R-ICA = internal carotid artery, R-MCA = right middle cerebral artery, VRT = volume-rendering technique.

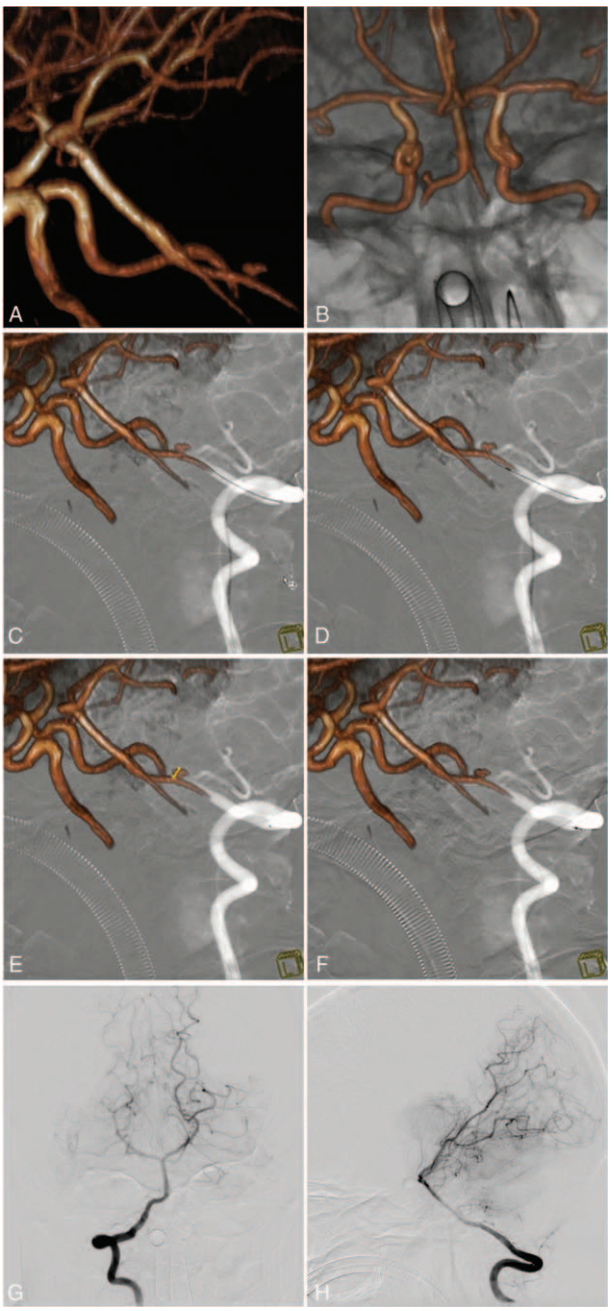

Figure 3. Magnetic resonance angiography (MRA) of the intracranial vessel (A); MRA overlaid with live fluoroscopy (B); with the MRA roadmap guidance, the guide wire entered R-VA (C), and approached the aneurysm neck (D); the aneurysm size was measured (E), and coiling was performed (F). Final DSA check of the coiling results in AP (G) and lateral (H) view. DSA = digital subtracted angiography.

(2 mm) and its parent artery (i.e., right vertebral artery). The vasculature presented by MRA (Fig. 3A) was overlaid with 2D live fluoroscopy (Fig. 3B). The MRA was used to select the best working angle, and then navigated the guide wire progression through the right vertebral artery into the V4 segment (Fig. 3C), which finally approached the aneurysm neck (Fig. 3D). The 3D MRA was found to precisely superimpose with the 2D color-inverted DSA roadmap of the target vessel obtained with 5 mL contrast medium injection. The 3D MRA revealed the size of the aneurysm for coil selection (Fig. 3E). Next, 3 coils (2.5 mm × 4 mm, 2 mm × 2 mm, 1 mm × 2 mm; MicroPlex 10, MicroVention) were carefully implanted and packed into the aneurysm sac through a microcatheter (Fig. 3F). A final DSA acquired with 5 mL contrast medium injection confirmed complete occlusion of the aneurysm (Fig. 3G, H). In our medical center, the aneurysm treatment typically involves 50 to 70 mL contrast medium and 1100 to 1900 mGy x-ray dose for an average coiling procedure without a MRA roadmap. When guided by the 3D MRA roadmap, however, the contrast medium injected was reduced to about 20 mL and the overall x-ray dose to patients to about 768 mGy.

3.2. Representative case 2

The second representative case was shown in Fig. 4 that demonstrated the treatment procedure of a severe basilar artery (BA) stenosis guided by the MRA roadmap. In Fig. 4A, MRA image showed the anatomy of a stenosis at BA and indicated the best working angle. During the endovascular procedures, the MRA was registered with the low-dose angiography of the skull, and then overlaid with 2D live fluoroscopy to provide intra-procedural guidance (Fig. 4B). The guide wire was first navigated into the left vertebral artery (VA) and then approached the proximal of the stenosis (Fig. 4C). The wire was further advanced through the tight lesion to reach the distal segment (Fig. 4D) and entered right posterior cerebral artery (PCA) afterwards (Fig. 4E). A balloon (2.5 mm × 9.0 mm; Maverick Monorail, Boston Scientific Scimed) was placed to predilate the stenosis (Fig. 4F). Next, an intracranial balloon-expandable stent (3.0 mm × 13 mm; Apollo, MicroPort Medical, China) was delivered across the stenosis (Fig. 4G) and deployed (Fig. 4H). The final DSA was acquired with 5 mL contrast medium injection each, and it confirmed successful recanalization of the VA from both anterior-posterior and lateral positions (Fig. 4I, J). With the use of 3D MRA roadmap, the overall amount of contrast medium used was decreased to only 30 mL, and x-ray dose was decreased to 1094 mGy (as compared with 50 to 90 mL contrast medium and 1300 to 2100 mGy x-ray dose used on average for a typical intracranial stenting procedure in the absence of the MRA roadmap guidance).

4. Discussion

Magnetic resonance angiography has shown to be an alternative to conventional angiography with an excellent diagnostic accuracy for neurovascular diseases. In the current study, we demonstrated that the CBCT-based dynamic 3D road mapping enabled registration of preprocedural MRA image with intraprocedural angiography, and overlay of 3D fusion images with real-time 2D fluoroscopy. We achieved precision in the registration of the 2 image modalities in all 19 patients from the first group. The 3D DSA images accurately superimposed onto the corresponding MRA images and enhanced visualization of vessels.

In the representative endovascular coiling case, the MRA informed a small aneurysm of exact size and location that was confirmed by 2D DSA. The 3D MRA roadmap enabled monitoring of the packing density and morphology of the coils from multiple angles, such that avoided coil prolapsing into parent vessel or protruding through aneurysm sac. Either scenario could lead to serious adverse neurological effects. Minor difference in posterior inferior cerebella artery (PICA) was visible only in the DSA image. The difference could be due to the fact that the aneurysm was located at the origin of the PICA. The MRA was performed in the acute phase of hemorrhage. This

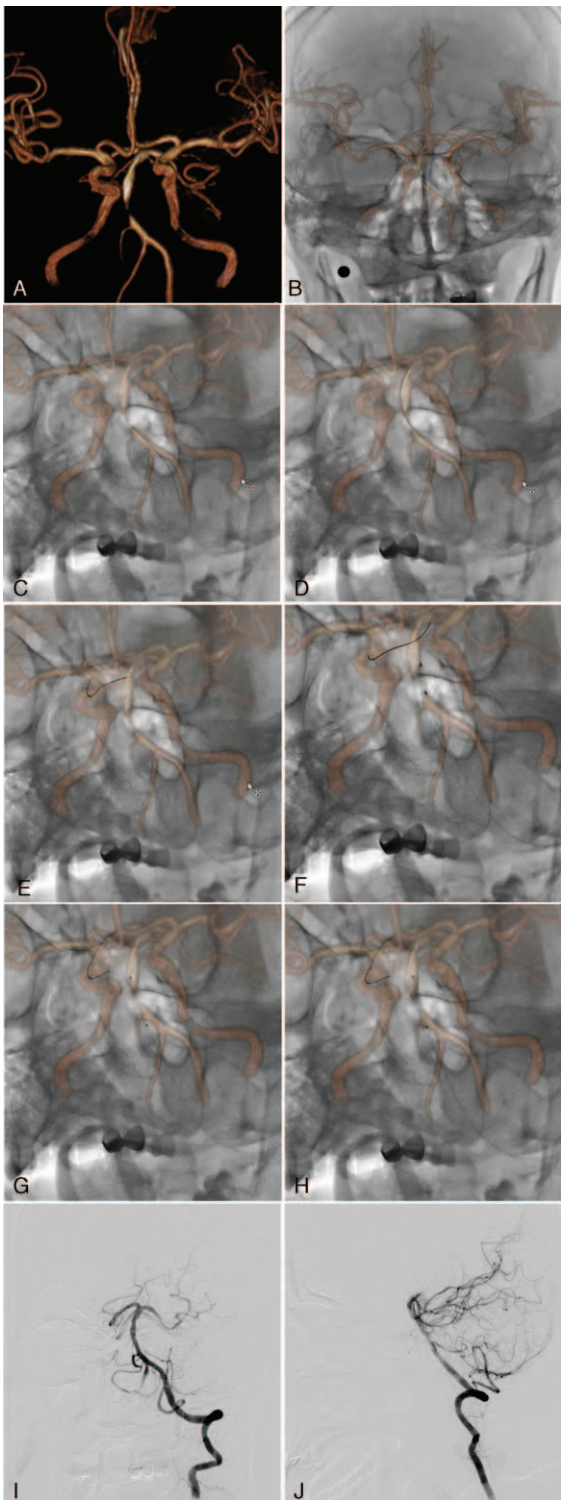

Figure 4. Preprocedural MRA showed severe BA stenosis (A). MRA was overlaid with live fluoroscopy (B). With 3D MRA roadmap, the guide wire entered left VA and approached the proximal of stenosis (C); the guide wire passed through the stenosis into distal segment (D) and then entered right PCA (E). A balloon was used for predilation of the stenosis (F). A intracranial stent was inserted across the stenosis (G) and expanded by the balloon (H). Final DSA check of the stenting result in AP (I) and lateral (J) view. 3D = 3-dimensional, DSA = digital subtracted angiography, MRA = magnetic resonance angiography, PCA = posterior cerebral artery, VA = vertebral artery.

stage of hemorrhage may cause vasospasm and reduce blood flow into the PICA. On the other hand, the DSA acquisition and the treatment were performed after the 2-day antispastic therapy, and conceivably, the PICA could be observed in the DSA image, but not in the MRA. In the stenosis stenting case, the lesion was accurately depicted by the MRA. The 3D MRA roadmap provided reliable guidance for the entire procedure including wire/catheter progression, stenosis predilation with balloon, and stent deployment. Slight arterial distortion was observed after endovascular device insertion, and minor deviation was in turn detected by comparing the marker positions of the balloon and stent in relation to the 3D MRA roadmap coordinates. In such cases, intraprocedural DSA may be required to update vasculature morphology.

In this study, the accuracy between 3D MRA and angiographic image fusion has been validated, and its advantages for guiding cerebral endovascular procedures have been also demonstrated. We showed that it is entirely possible to substantially reduce radiation dose and renal load of patients without compromising either examination or treatment. MRI has become a noninvasive routine component in the imaging assessment of patients with neurovascular diseases. The key benefit of this approach lies in the readily available preprocedural MRA images that provide 3D information for endovascular procedures. This eliminates the repetitive acquisition of 3D DSA of the target vessels and simplifies workflow. Because the MRA is registered to the low-dose 3D angiography and then overlaid to live 2D fluoroscopy as real-time guidance, the endovascular procedures are therefore performed with possible minimum use of contrast medium. Consequently, this approach is uniquely valuable for applications in young patients or in those with renal impairment. Moreover, since the procedures can be performed mainly under fluoroscopy, x-ray dose to patient can in turn be greatly reduced.

The image fusion technique allows clear visualization of vasculature of interest in 3D space from any desired angle during endovascular procedures to aid in choices of the best working angle. It also helps verify the wire tip position during its advancement within the vessel lumen as guided by the 3D MRA roadmap. As such, this approach can be rather useful in the case of arterial occlusion, where distal segment of the occlusion is often invisible in DSA images due to contrast medium blockage. In contrast to DSA method, the MRA could provide sufficient visualization of the distal segment of the occlusion, and thus, accurate localization of the wire/catheter position with respect to the 3D anatomical structure including the occluded vessel segment. The procedure-related complications may in turn be reduced.[11,20]

Owing to the limited spatial resolution of MRI, imaging small vessels such as perforating arteries remains challenging. To achieve proper 3D fusion between the MRA and angiography, subsequent overlay with live 2D fluoroscopy images, and accurate production of final image roadmaps, the patient should be stabilized to minimize unanticipated movement that might result in misalignment during image registration. Otherwise, precision of intraprocedural guidance may be compromised. Besides, although this approach can significantly reduce contrast medium usage added by performing 2D and 3D DSA of the vessel, due to the limited imaging field of MRA using head coils, only intracranial vessels are acquired and used to guide for endovascular procedures. To address this issue, our current workflow still involves certain amount of contrast medium injection during catheterization and wire progression to assist fine selection of artery with lesions. Future MRA of the head and

neck region requires improvement in sensitivity and coverage of vessels. The 3D MRA-associated roadmap of entire cerebral circulation is warranted to help further reduce or even eliminate the contrast medium usage during endovascular procedures and enhance operation safety. Currently, another limitation is that the MRA examination time is longer than that typically required for CTA. Acquiring MRA could then be difficult in acute cases, and MRA applications may be questionable in such patient cohorts. Worthy of note, patients with implants such as pacemakers should be considered carefully as they might be affected by the strong magnetic field with MRA. Since our study did not enroll a large number of patients, future investigations of larger-size patient populations are needed to further evaluate clinical applications of the fusion method.

5. Conclusions

The current work demonstrated successful fusion between 3D MRA and angiographic images for accurate visualization of cerebral vasculature. The use of MRA image as 3D roadmap was shown to be both feasible and excellent to guide endovascular procedures. The fusion approach may enhance clinical workflow while reducing radiation dose to patients and contrast medium usage. The method offers important clinical value in lowering endovascular procedure risks and increasing treatment safety.

References

[1] Siewerdsen JH, Moseley D, Burch S, et al. Volume CT with a flat-panel detector on a mobile, isocentric C-arm: pre-clinical investigation in guidance of minimally invasive surgery. Med Phys 2005;32:241–54.
[2] Benndorf G, Klucznik RP, Strother CM. Images in cardiovascular medicine. Angiographic computed tomography for imaging of under deployed intracranial stent. Circulation 2006;114:e499–500.
[3] Engelhorn T, Struffert T, Richter G, et al. Flat panel detector angiographic CT in the management of aneurysmal rupture during coil embolization. AJNR Am J Neuroradiol 2008;29:1581–4.
[4] Akpek S, Brunner T, Benndorf G, et al. Three-dimensional imaging and cone beam volume CT in C-arm angiography with flat panel detector. Diagn Interv Radiol 2005;11:10–3.
[5] Heran NS, Song JK, Namba K, et al. The utility of DynaCT in neuro endovascular procedures. AJNR Am J Neuroradiol 2006;27:330–2.
[6] White PM, Gilmour JN, Weir NW, et al. AngioCT in the management of neuro interventional patients: a prospective, consecutive series with associated dosimetry and resolution data. Neuroradiology 2008;50: 321–30.
[7] Hankey GJ, Warlow CP, Sellar RJ. Cerebral angiographic risk in mild cerebrovascular disease. Stroke 1990;21:209–22.
[8] Katzberg RW. New and old contrast agents: physiology and nephrotoxicity. Urol Rad 1988;10:6–11.
[9] Byrd L, Sherman RL. Radiocontrast induced acute renal failure: a clinical and pathophysiologic review. Medicine 1979;58:270–9.
[10] Berns AS. Nephrotoxicity of contrast material. Kidney Int 1989;36: 730–40.
[11] Raval AN, Karmarkar PV, Guttman MA, et al. Real-time magnetic resonance imaging-guided endovascular recanalization of chronic total arterial occlusion in a swine model. Circulation 2006;113: 1101–7.
[12] Zhang Z, Fan Z, Carroll TJ, et al. Three-dimensional T2-weighted MRI of the human femoral arterial vessel wall at 3.0 Tesla. Invest Radiol 2009;44:619–26.
[13] Lippincott Williams & Wilkins, Hashemi RH, Bradley WG, Lisanti CJ. MRI: The Basics, Chapter 1. 3rd ed2010;310–326.
[14] Uchida M, Ishibashi M, Tomita N, et al. Hilar and suprapancreatic cholangiocarcinoma: value of 3D angiography and multiphase fusion images using MDCT. AJR Am J Roentgenol 2005;184:1572–7.
[15] Ide S, Hirai T, Morioka M, et al. Usefulness of 3D DSA-MR fusion imaging in the pretreatment evaluation of brain arteriovenous malformation. Acad Radiol 2012;19:1345–52.
[16] Hamm KD, Klisch J, Surber G, et al. Special aspects of diagnostic imaging for radiosurgery of arteriovenous malformations. Neurosurgery 2008;62 (5 suppl):A44–52.
[17] Faragò G, Caldiera V, Tempra G, et al. Advanced digital subtraction angiography and MR fusion imaging protocol applied to accurate placement of flow diverter device. J Neurointerv Surg 2016;8:e5.
[18] Suzuki H, Shimizu S, Maki H, et al. Role of image fusion combining three-dimensional digital subtraction angiography with magnetic resonance imaging in evaluation of unruptured cerebral aneurysms. Neurol Res 2007;29:58–63.
[19] Sheng L, Li J, Li H, et al. Evaluation of cerebral arteriovenous malformation using 'dual vessel fusion' technology. J Neurointerv Surg 2014;6:667–71.
[20] Klein AJ, Tomkowiak MT, Vigen KK, et al. Multi-modality image fusion to guide peripheral artery chronic total arterial occlusion recanalization in a swine carotid artery occlusion model: unblinding the interventionalist!. Catheter Cardiovasc Interv 2012;80:1090–8.